Biochimica et Biophysica Acta, 974 (1989) 149–155
Elsevier

BBA 42974

Electron spin polarization of P^+-870Q^- observed in the reaction center protein of the photosynthetic bacterium *Rhodobacter sphaeroides* R-26. The effect of selective isotopic substitution at X- and Q-band microwave frequencies *

L.L. Feezel [1], P. Gast [2,**], U.H. Smith [1] and M.C. Thurnauer [1]

[1] *Chemistry Division, Argonne National Laboratory, Argonne, and* [2] *Department of Chemistry, The University of Chicago, Chicago, IL (U.S.A.)*

(Received 8 September 1988)

Key words: Electron spin polarization; ESR; Reaction center; Photosynthesis; Deuteration; (*Rb. sphaeroides*)

The X-band (9.5 GHz) electron spin polarized (ESP) electron paramagnetic resonance (EPR) signal observed in iron-depleted bacterial reaction centers is due to P^+-870Q^- (P^+-870 is the oxidized primary donor, a special pair of bacteriochlorophyll molecules, and Q^- is the reduced primary quinone acceptor). This signal contains information about the dynamic interactions and spatial relationships between the photosynthetic primary reactants as they undergo electron transfer. Interpretations of the X-band ESP EPR spectrum have not been unique because of insufficient spectral resolution and the simulations require a large number of adjustable parameters. Therefore, we have acquired ESP EPR spectra at X-band and Q-band (35 GHz) from iron-depleted bacterial reaction centers in which P-870, I (intermediary bacteriopheophytin acceptor), and Q were selectively deuterated (protonated). The effects of selective isotopic substitution and microwave frequency on the ESP EPR spectra of P^+-870Q^- (i) could not be explained by the polarization transfer mechanism alone, and (ii) allowed the determination of the polarization contributions of ^{2}(P^+-870) and ^{2}(Q^-) to the composite ESP EPR spectrum. The resolution of these components suggests that the spin-correlated radical pair mechanism makes a significant contribution to the ESP spectrum from ^{2}(P-870I)^{2}Q. The results presented here should provide a stringent test for computer simulations of the correct mechanism of ESP production.

Introduction

The study of transient radicals by time-resolved electron paramagnetic resonance (EPR) methods gives rise in most instances to spectra which exhibit electron spin polarization (ESP), or a non-Boltzmann spin population distribution. The observation and subsequent understanding of this phenomenon is an important tool to study dynamic interactions between transient radicals (Refs. 1 and 2; for general references, see in particular Ref. 1). Thus, the observations of ESP from radicals with resonances near $g = 2$ *** initially in green plant photosystem I [6] and subsequently in photosynthetic bacterial reaction centers (RCs) [7] should provide insight into the nature and magnitude of the interactions as well as the spatial relationships between the photosynthetic primary reactants as they undergo electron transfer. Yet, mechanisms used to interpret the ESP spectra from photosynthetic systems have been only moderately successful. In the case of the ESP spectra from the bacterial RCs, problems in interpretations are

** Present address: The University of Connecticut, Storrs, CT 06268, U.S.A.

*** This distinction is made to differentiate the ESP described here from that due to the photoexcited triplet state of the primary donor observed initially in bacterial reaction centers [3] and later in green plant Photosystems I [4,5] and II [36].

Abbreviations; ESP, electron spin polarization; EPR, electron paramagnetic resonance; I, intermediary bacteriopheophytin acceptor; *D*, dipolar interaction parameter; *J*, exchange coupling parameter.

Correspondence: M.C. Thurnauer, Chemistry Division, Argonne National Laboratory, 9700 South Cass Avenue, Argonne, IL 60439, U.S.A.

primarily due to insufficient spectral resolution; whereas in green plant PS I these difficulties are due to lack of understanding of the primary reactants.

The observation of ESP, using conventional X-band (9.5 GHz) EPR, from photosynthetic bacterial RCs was first reported by Hoff et al. [7]. The transient ESP signal was only observed in iron-depleted RCs. The authors suggested that the signal was due to P^+-870Q^- (P^+-870 is the oxidized primary donor, a special pair of bacteriochlorophyll molecules, and Q^- is the reduced primary quinone acceptor). Further refinement of the experiment demonstrated that this was indeed the case and that the polarization pattern of the composite spectrum which was observed at short times with respect to the exciting pulse is low-field emission, middle-field enhanced absorption, high-field emission [8,9]. The 'three-lobed' polarization pattern of a radical pair formed by two sequential electron transfer steps

$$\text{P-870IQ} \xrightarrow{h\nu} \text{P}^+\text{-870I}^-\text{Q} \rightarrow \text{P}^+\text{-870IQ}^-$$

(I is the intermediary bacteriopheophytin acceptor) could be simulated using the mechanism involving polarization transfer first proposed by Pedersen [10]. In this mechanism, ESP observed in P^+-870 and Q^- reflects only P^+-870I^- radical pair interactions. P^+-870 and Q^- are not interacting. The simulations [8,9] require that the polarization contribution of P^+-870 to the spectrum be A^*/E (low-field enhanced absorption/high-field emission with excess absorption from the so-called 'net effect' symbolized by *). However, some of the parameters chosen to obtain a best fit to the experimental spectrum deviated considerably from the accepted values.

The same 'three-lobed' ESP EPR spectrum has been observed from reactions of green plant Photosystem I [11–14,37–45] and interpreted by more than one model. The most generally applied model includes the polarization transfer mechanism [8,14,43–45]. However, studying this signal in fully deuterated systems at higher microwave frequencies (K-band (24 GHz) and Q-band (35 GHz)) [15–17], demonstrated that the X-band 'three-lobed' composite spectrum cannot be modeled by the simple polarization-transfer mechanism.

In other attempts to simulate the ESP spectra from the bacterial RCs and green plant Photosystem I, the polarization-transfer mechanism was used with incorporation of anisotropic terms [18]. In the case of bacterial RCs, the anisotropic terms included were dipolar interaction in the first pair, P^+-870I^-, and an anisotropic g-tensor for Q^-. The result required that the polarization contribution of P^+-870 was A/E^* in contrast to the previous interpretation [8,9]. Note that both interpretations [8,9,18] differ from the results of recent EPR experiments on iron-containing RCs in which the native quinone has been replaced by different quinones. In these experiments, Gunner et al. [19] observed a transient spin-polarized signal that had a low-field emissive and a high-field absorptive component and assigned it to P^+-870.

Recently, the problems encountered in interpretations of the ESP spectrum observed in iron-depleted bacterial RCs have been noted [20]. Among these are: (i) the requirement for a large ratio, D/J (D is the dipolar interaction parameter and J is the exchange coupling parameter in the P^+-870I^- pair); (ii) a relatively large absolute value for J; and (iii) the deviation from accepted values for some of the g-factors and linewidths used as input. Therefore, another approach has been applied. This model is based on an ESP mechanism which has been used to explain an unexpected electron spin echo phase shift of the ESP signals observed by pulsed EPR in green plant Photosystem I [40] and photoreactions in micelles [21]. Recently, quantitative descriptions of this model have been presented to explain the unusual features present in the ESP EPR spectra of photoreactions in micelles [22,23] and biradicals [24]. Using this approach, Hore et al. [20] simulated the ESP observed in the iron-depleted bacterial RCs, with the assumption that the intermediate pair P^+-870I^- is too short-lived to contribute to development of ESP. Thus the ESP in P^+-870Q^- results from rapid formation of this spin-correlated radical pair. Although the results are promising, the initial assumption may conflict with the experimental results of Gunner et al. [19] which demonstrated that polarization of P^+-870 is only observed in those RCs in which the particular quinone substitution increases the lifetime of P^+-870I^- relative to that in native RCs. Also, iron depletion might increase the lifetime of P^+-870I^- relative to its lifetime in native RCs [25,47].

Clearly, a simulation of the X-band ESP EPR spectrum of bacterial RCs will not be unique because of insufficient spectral resolution and the number of adjustable parameters needed to describe ESP. Therefore, to aid in the determination of the correct mechanism of ESP observed from P^+-870Q^- in bacterial RCs, we have measured ESP EPR spectra at X-band and Q-band microwave frequencies from iron-depleted RCs in which P-870, I, and Q were selectively deuterated (protonated). The corresponding change in linewidth upon deuteration (protonation) and increased spectral resolution at Q-band microwave frequency allow the origin of several features of the ESP spectrum to be determined.

Materials and Methods

Reaction centers from the photosynthetic bacterium, *Rhodobacter sphaeroides* R-26 were isolated according to the procedures described by Wraight [26]. The method of Tiede and Dutton [27] was followed for removal of Fe from the reaction centers. Deuterated reaction centers

were isolated from whole cells of *Rb. sphaeroides* R-26 which were grown in D_2O (99.7%) on deuterated substrates [28,48]. Deuterated ubiquinone-10 was obtained from these cells using the method of Hale et al. [29]. Quinone removal and reconstitution with deuterated or protonated ubiquinone-10 was done according to Okamura et al. [30]. The extent of quinone removal and reconstitution was tested by measuring the amplitudes of the EPR signals of P^+-870 and ^{3}P-870. These measurements indicated that more than 90% of the quinone was removed and that 90% was reconstituted. Reaction center samples used in the EPR experiments contained approx. 50% ethylene glycol and were frozen (77 K) in the dark. The samples were checked by EPR for the presence of any reduced quinone in the dark before and after illumination, since spin polarized signals from chemically prereduced quinone have been observed in such systems [8] and could interfere with the ESP spectrum of P^+-870Q^-. No EPR signal was observed without illumination.

Samples of the following isotopic composition were used:

(a) protonated reaction centers ^{1}(P-870I)^{1}Q;
(b) deuterated reaction centers ^{2}(P-870I)^{2}Q;
(c) protonated reaction centers with deuterated ubiquinone-10 ^{1}(P-870I)^{2}Q;
(d) deuterated reaction centers with protonated ubiquinone-10 ^{2}(P-870I)^{1}Q.

The low temperature X-band EPR experiment and light modulation (500 Hz) experiment combined with phase-sensitive detection have been described previously [16]. The Q-band EPR spectra were recorded using a Bruker ER053QRD Q-band EPR bridge, a Varian TE_{011} cavity and a Varian E-9 series console. For low-temperature Q-band EPR experiments, the EPR cavity was placed inside an Air products LTR cryostat in which the X-band dewar was replaced with a wide mouthed dewar. Temperatures at the sample position in the cavity (see figure captions) were measured with a chromel vs. gold (0.07% iron) thermocouple inserted in an EPR tube filled with water.

The *g*-factors were determined by comparison to a standard Varian strong pitch sample ($g = 2.0028$) at X-band and to the light induced signal of P^+-870 ($g = 2.0026$) [31] in protonated native reaction centers of *Rb. sphaeroides* R-26 at Q-band. The errors in the measured *g*-factors are ± 0.0004 (2 standard deviations).

Since the experimental ESP EPR spectra are obtained using a modulated light source combined with phase-sensitive detection of the EPR signal with respect to the light source, phase problems can result. In the experiments reported here, all signals were phased for maximum amplitude and in several instances (see Results section) we were able to verify that the light-modulated ESP EPR signal is the same as that obtained at early times with more direct time-resolved EPR methods [8,9,17]. Relative spectral intensities within a given ESP EPR signal did not change with the modulation frequency (100 Hz to 1 kHz) of the light source. For each sample, no EPR signal was observed 90° out of phase except when the ^{2}(P-870I)^{1}Q sample was studied. The sense of the polarization (absorption vs. emission) was calibrated by reference to the polarized triplet EPR spectrum observed in the reaction centers.

Results

Rb. sphaeroides R-26 reaction centers of various isotopic composition were studied using X-band and Q-band EPR. The EPR signals measured under continuous illumination and with light modulation (ESP EPR signals) are displayed in Figs. 1 and 2.

X-band continuous illumination

The spectrum obtained from ^{1}(P-870I)^{1}Q (Fig. 1a) has a *g*-factor of 2.0033 and the lineshape is characteristic of the composite spectrum reported for P^+-870Q^- [8,32]. ^{2}(P-870I)^{2}Q gives a spectrum (Fig. 1b) that shows partial low-field spectral resolution and clearly reveals the presence of Q^- in the spectrum.

X-band light modulation

The ESP EPR spectrum (Fig. 1a) obtained from ^{1}(P-870I)^{1}Q shows the same features (E/A/E and *g*-factors) as those studied using more direct time resolved EPR methods [8,9,17]. This comparison verifies the light modulation technique and the sense of the polarization. The ESP EPR spectrum (Fig. 1b) obtained from ^{2}(P-870I)^{2}Q shows an absorptive feature at $g = 2.0003$ which is not apparent in the ESP EPR spectrum obtained from ^{1}(P-870I)^{1}Q (Fig. 1a) or ^{1}(P-870I)^{2}Q (Fig. 1c).

Q-band continuous illumination

Each Q-band EPR spectrum (Fig. 2) obtained under continuous illumination is better resolved than at X-band showing a low field peak which is due to Q^- and a high field absorption at $g = 2.0025$ which is due to the superposition of the spectra of P^+-870 and Q^- [33]. The relative intensity of the low-field peak to that of the high-field peak varies with isotopic substitution. Powder spectrum simulations showed that the observed relative intensity of the low-to-high field peak is as expected. Thus, the signals are not microwave power saturated and there are no contributions to the spectrum from RCs that contain iron. In the spectra obtained from ^{2}(P-870I)^{2}Q and ^{1}(P-870I)^{2}Q (Fig. 2b and c), the low-field absorption is partially resolved showing the *g*-anisotropy of Q^- ($g_{xx} = 2.0068$, $g_{yy} = 2.0056$, $g_{zz} = 2.0024$) [8,33].

Q-band light modulation

The ESP EPR spectrum obtained from ^{1}(P-870I)^{1}Q (Fig. 2a) shows similar features as the K-band ESP EPR

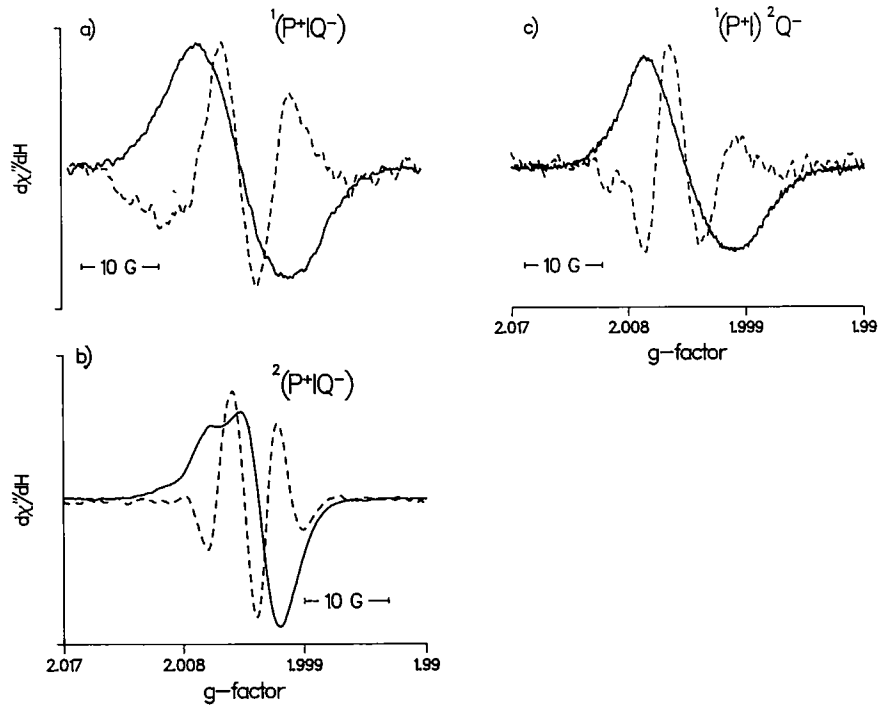

Fig. 1. X-band EPR signals measured under continuous illumination (———) and with 500 Hz light modulation (- - - - - -). Microwave power, 0.01 mW; 100 kHz field modulation; temperature 8 K. (a) ^{1}(P-870I)^{1}Q modulation amplitude, 1.0 gauss. (b) ^{2}(P-870I)^{2}Q modulation amplitude, 0.5 gauss. (c) ^{1}(P-870I)^{2}Q modulation amplitude, 0.5 gauss. (Each spectrum is plotted so that the peak with maximum amplitude is full scale.)

spectrum of Petersen et al. [17]. Additional spectral resolution is observed with deuterated samples at Q-band (Fig. 2b). An emissive feature is predominant at low field while at high field both absorptive and emissive features are major components. The ESP EPR spectrum of ^{1}(P-870I)^{2}Q (Fig. 2c) shows a low-field emissive feature with the same g-factor (2.0056) and linewidth as the low-field emissive feature of the spec-

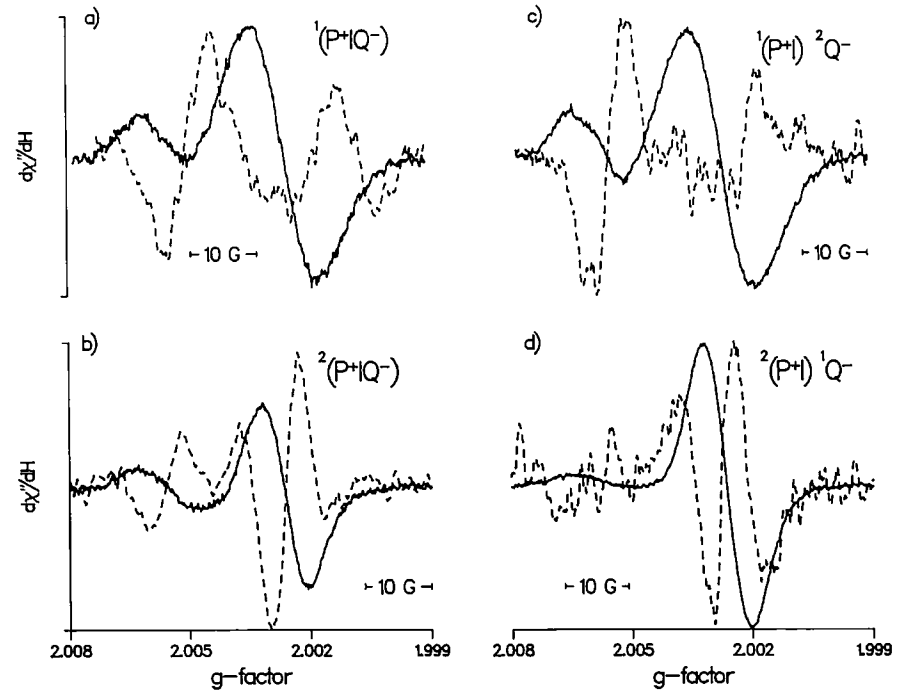

Fig. 2. Q-band EPR signals measured under continuous illumination (———) and with 500 Hz light modulation (- - - - -). Modulation amplitude 6 gauss, 100 kHz field modulation; temperature 30 K. (a) ^{1}(P-870I)^{1}Q Microwave power, 0.24 μW. (b) ^{2}(P-870I)^{2}Q Microwave power, 0.24 μW. (c) ^{1}(P-870I)^{2}Q Microwave power, 2.4 μW. (d) ^{2}(P-870I)^{1}Q Microwave power, 24 μW. (Each spectrum is plotted so that the peak with maximum amplitude is full scale.)

trum from ^{2}(P-870I)^{2}Q (Fig. 2b). At high field the spectrum differs from that of Fig. 2b; a single spectral feature at $g = 2.0018$ is present. The ESP EPR spectrum of ^{2}(P-870I)^{1}Q (Fig. 2d) has major features at g-factors that overlap the high-field portion of the spectrum obtained from ^{2}(P-870I)^{2}Q (Fig. 2b).

Discussion

Comparing the EPR spectra obtained from samples which differ only in isotopic composition as well as observing them at different microwave frequencies is often used to resolve EPR spectra which are made up of more than one radical or a radical exhibiting g-anisotropy. This technique is also useful in determining which magnetic interactions give rise to spectral splittings. Zeeman interactions (g-factors) are frequency dependent and electron-nuclear hyperfine interactions depend on isotopic composition. Electron–electron couplings do not vary with either frequency or isotope. When EPR spectra show electron spin polarization, the pattern of ESP depends on the relative magnitudes of the same interactions. Therefore, the observation of changes in the ESP EPR spectra as a function of isotopic composition and microwave frequency can be a way to understand the mechanism of ESP production.

In the P$^+$-870Q$^-$ ESP EPR signal, we expect that the magnitudes of several of the magnetic interactions which contribute to the spectral splittings and to the pattern of ESP are similar. Therefore, the observed ESP EPR spectrum will be due to a complex interplay of these interactions and ultimately requires a complete simulation to understand the mechanism of ESP radical pair production. Such a simulation should include a consideration of ESP development from both polarization transfer and rapid formation of a spin-correlated radical pair as well as parameters that are consistent with the known structure of the reaction center crystal. Nevertheless, by comparing the line splittings and polarization patterns of the experimental ESP EPR spectra as a function of frequency and isotopic composition, we can already make some conclusions about which magnetic interactions are significant and possible mechanisms for formation of ESP.

The polarization pattern $E/A/E$ for the X-band ESP EPR spectrum from ^{1}(P-870I)^{1}Q (Fig. 1a) that was first observed by Hoff et al. [7] changes to $E/A/E/A$ for the X-band ESP EPR spectrum from ^{2}(P-870I)^{2}Q (Fig. 1b). The appearance of the high-field absorption peak in the spectrum from ^{2}(P-870I)^{2}Q could be due simply to the fact that the unresolved hyperfine interactions which contribute to the linewidths are reduced sufficiently compared to those in ^{1}(P-870I)^{1}Q so that a splitting due to other interactions (exchange, dipolar, g-factor differences) is expressed. On the other hand, a reduction in hyperfine interactions relative to g-factor differences could cause a change in polarization even at X-band so that the high-field absorption appears. The former explanation seems most reasonable because the overall polarization pattern ($E/A/E/A$) from ^{2}(P-870I)^{2}Q does not change with microwave frequency (compare Fig. 1b with 2b). Similar explanations could be given for the observed change from $E/A/E$ to $E/A/E/A$ for ^{1}(P-870I)^{1}Q upon going from X-band to Q-band (compare Fig. 1a with 2a) except that instead of a reduction in hyperfine interactions there is an increase in the g-factor differences.

Although the overall ESP pattern in the ^{2}(P-870I)^{2}Q spectra is independent of the change in microwave frequency from X-band to Q-band, the separation between the low-field resonance (E) and the remaining resonances ($A/E/A$) (Figs. 1b and 2b) increases. This separation is frequency dependent and must be related to g-factor differences. We expect that these g-factor differences are between the low-field resonances of ubiquinone and those primarily due to P$^+$-870. Our assignment of the low-field resonance at $g_{yy} = 2.0056$ to ubiquinone is supported by comparison of the ^{2}(P-870I)^{2}Q ESP EPR spectrum (Fig. 2b) to the Q-band EPR signals obtained under continuous illumination (Fig. 2b and [33]) and from chemically reduced ubiquinone ($g_{xx} = 2.0068$, $g_{yy} = 2.0056$, $g_{zz} = 2.0024$). [8] This comparison also shows that the ESP EPR spectrum obtained from ^{2}(P-870I)^{2}Q (Fig. 2b) has no polarized feature at $g_{xx} = 2.0068$.

Differences are observed in the Q-band ESP EPR spectra obtained from ^{1}(P-870I)^{2}Q and ^{2}(P-870I)^{1}Q (Fig. 2c and d, respectively) which suggest that in each case the signal intensity of the protonated component is attenuated leaving only the ESP spectrum of the deuterated component. In Fig. 2c, the g-factors of the spectral features are in the range of the g-factors reported for ubiquinone [8,33] and the low-field feature has a similar g-factor and linewidth as the low field feature in the spectrum obtained from ^{2}(P-870I)^{2}Q. If we assume that the spectrum in Fig. 2c is the ubiquinone contribution to the ESP EPR composite spectrum, it is all in emission with an anisotropic polarization. This anisotropic polarization is different from that reported in RCs in which the ubiquinone was prereduced [8]. On the other hand, the ESP EPR spectrum obtained from ^{2}(P-870I)^{1}Q (Fig. 2d) is centered around $g = 2.0028$ and has features similar to the high-field peaks of the spectrum obtained from ^{2}(P-870I)^{2}Q. Thus, the spectral features of Fig. 2d appear to be due to deuterated P$^+$-870 making its contribution to the composite ESP EPR spectrum $A/E/A$. In fact, the addition of the spectra obtained from ^{1}(P-870I)^{2}Q (Fig. 2c) and ^{2}(P-870I)^{1}Q (Fig. 2d) gives a total spectrum (Fig. 3) very similar to that obtained from ^{2}(P-870I)^{2}Q.

One explanation for the attenuated spectral intensities of the protonated species in the ESP EPR spectra

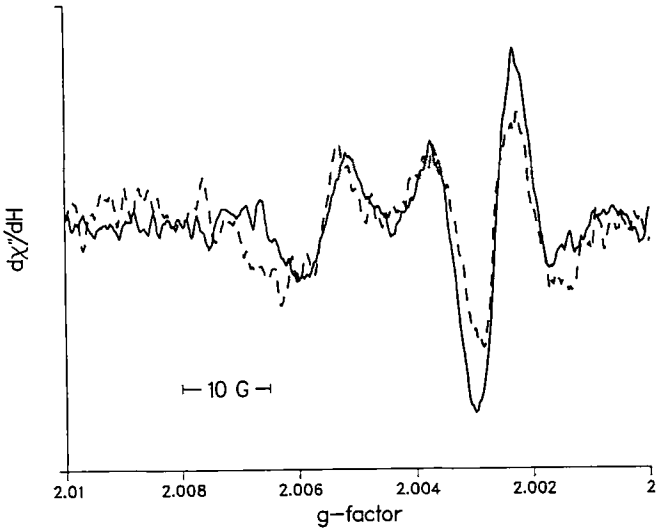

Fig. 3. Comparison of the Q-band EPR signal from ^{2}(P-870I)^{2}Q measured with 500 Hz light modulation (same as Fig. 2b) (———) and the sum of the Q-band EPR signals from ^{1}(P-870I)^{2}Q (same as Fig. 2c) and ^{2}(P-870I)^{1}Q (same as Fig. 2d) measured with 500 Hz light modulation. (- - - - -).

obtained from ^{1}(P-870I)^{2}Q and ^{2}(P-870I)^{1}Q (Fig. 2c and 2d) is that the spin-correlated radical-pair mechanism makes a significant contribution to the ESP. In this mechanism, a non-zero exchange or dipolar interaction in the radical pair being observed will cause each hyperfine transition to shift and split into a doublet with one emissive and one absorptive component [20,22–24,34,40]. Therefore, the attenuated intensities of the spectral features due to the protonated species in Fig. 2c and d could result from cancellation of overlapping absorption and emission lines. These cancellation effects would be diminished in spectra obtained from deuterated radicals because of narrower unresolved hyperfine interactions compared to protonated radicals.

If the spectrum shown in Fig. 2d is in fact the contribution of deuterated P^+-870 to the polarized spectra, then the *A/E/A* pattern obtained does not support the polarization transfer [8–10,18,43–46] mechanism of ESP radical pair production. As pointed out in the Introduction, simulations of the X-band ESP EPR spectrum using the mechanism of polarization transfer [8,9,18,46] required that the polarization contribution of P^+-870 be *A*/E* or *A/E** (if dipolar interaction in P^+-870I$^-$ and *g*-anisotropy of Q^- is included). This same model would predict that at Q-band the polarization contribution of P^+-870 would show predominantly net polarization (*A* or *E*, respectively) and this is not observed [44]. Thus, the mechanism of polarization transfer by itself is not sufficient to reproduce the spectra obtained in this work.

The *A/E/A* polarization pattern for deuterated P^+-870 differs from the *E/A* P^+-870 polarization reported by Gunner et al. [19]. The latter X-band EPR experiments were done with native protonated reaction centers (Fe present) in which different types of quinone were substituted for the native ubiquinone. However, from the protonated systems studied in this work, we cannot exclude the possibility that the polarization contribution of ^{1}(P^+-870) is *E/A* and differs from the polarization contribution of ^{2}(P^+-870).

In summary, the effects of selective isotopic substitution and microwave frequency on the ESP EPR spectra of P^+-870Q^- have allowed us to determine (i) that the polarization transfer mechanism alone cannot account for the fact that the composite ESP EPR spectrum from ^{2}(P-870I)^{2}Q does not change with microwave frequency and that the ^{2}(P^+-870) polarization contribution does not show a predominant 'net' polarization at Q-band; and (ii) that the polarization contribution of ^{2}(P^+-870) to the composite ESP EPR spectrum is *A/E/A* and the contribution of ^{2}(Q^-) is all emission with an anisotropic polarization (absence of feature at $g_{xx} = 2.0068$). The resolution of the ^{2}(P^+-870) and ^{2}(Q^-) polarization contributions to the composite spectrum may be indicative of a significant contribution of the spin-correlated radical-pair mechanism to the ESP. Although these results strongly suggest that magnetic interactions between P^+-870 and Q^- are required for ESP production, they cannot be used to determine whether P^+-870I$^-$ interactions contribute to ESP development. Computer simulations are being carried out to investigate the possibility that both the polarization transfer mechanism and the spin-correlated radical-pair mechanism contribute to the ESP. The X-band and Q-band ESP EPR spectra presented in Figs. 1 and 2 with the published X-band [7–9] and K-band [17] ESP EPR spectra obtained from protonated reaction centers should provide a stringent test for the computer simulations of the correct mechanism of ESP radical pair production in photosynthetic bacteria.

Acknowledgements

This work was supported by the U.S. Department of Energy, Office of Basic Energy Sciences, Division of Chemical Sciences under contract W-31-109-Eng-38. Preliminary Q-band data were obtained at the National Biomedical EPR Center, Milwaukee, Wisconsin with the assistance of C. Felix and J. Hyde. We thank J.R. Norris, A.L. Morris, and D.E. Budil for many beneficial discussions. A. Kostka's technical assistance is appreciated. We acknowledge J. Gregar for constructing the cryostat dewar for Q-band measurements.

References

1 Muus, L.T., Atkins, P.W., McLauchlan, K.A. and Pedersen, J.B. (eds.) (1977) Chemically Induced Magnetic Polarization, Theory, Technique, and Applications, D. Reidel, Dordrecht.

2 Hoff, A.J. (1984) Q. Rev. Biophys. 7, 153–282.
3 Dutton, P.L., Leigh, J.S. and Seibert, M. (1972) Biochem. Biophys. Res. Comm. 46, 406–415.
4 Frank, H.A., McLean, M.B. and Sauer, K. (1979) Proc. Natl. Acad. Sci. USA 76, 5124–5128.
5 Rutherford, A.W. and Mullet, J.A. (1981) Biochim. Biophys. Acta 635, 225–235.
6 Blankenship, R.E., McGuire, A. and Sauer, K. (1975) Proc. Natl. Acad. Sci. USA 72, 4943–4947.
7 Hoff, A.J., Gast, P. and Romijn, J.C. (1977) FEBS Lett. 73, 185–190.
8 Gast, P. (1982) Thesis, University of Leiden, Leiden.
9 De Groot, A., Gast, P. and Hoff, A.J. (1984) in: Advances in Photosynthesis Research, (Sybesma, C., ed.), Vol. I, pp. 215–218, Martinus Nijhoff/Dr. W. Junk Publishers, Dordrecht.
10 Pedersen, J.B. (1979) FEBS Lett. 97, 305–310.
11 McIntosh, A.R., Manikowski, H., Wang, S.K., Taylor, G.P.S. and Bolton, J.R. (1979) Biochem. Biophys. Res. Comm. 87, 605–612.
12 Thurnauer, M.C., Bowman, M.K. and Norris, J.R. (1979) FEBS Lett. 100, 309–312.
13 McCracken, J.L., Frank, H.A. and Sauer, K. (1982) Biochim. Biophys. Acta 679, 156–168.
14 Gast, P., Swarthoff, T., Ebskamp, F.C.R. and Hoff, A.J. (1983) Biochim. Biophys. Acta 722, 163–175.
15 Furrer, R. and Thurnauer, M.C. (1983) FEBS Lett. 153, 399–403.
16 Thurnauer, M.C. and Gast, P. (1985) Photobiochem. Photobiophys. 9, 29–38.
17 Petersen, J., Stehlik, D., Gast, P. and Thurnauer, M. (1987) Photosynth. Res. 14, 15–29.
18 Hore, P.J., Watson, E.T., Pedersen, J.B. and Hoff, A.J. (1986) Biochim. Biophys. Acta 849, 70–76.
19 Gunner, M.R., Robertson, D.E., LoBrutto, R.L., McLaughlin, A.L. and Dutton, P.L. (1987) in Progress in Photosynthesis Research (Biggins, J., ed.), Vol. I, pp. 217–220, Martinus Nijhoff, Dordrecht.
20 Hore, P.J., Hunter, D.A., McKie, C.D. and Hoff, A.J. (1987) Chem. Phys. Lett. 137, 495–500.
21 Thurnauer, M.C. and Meisel, D. (1983) J. Am. Chem. Soc. 105, 3729–3731.
22 Closs, G.L., Forbes, M.D.E. and Norris, J.R. (1987) J. Phys. Chem. 91, 3592–3599.
23 Buckley, C.D., Hunter, D.A., Hore, P.J. and McLauchlan, K.A. (1987) Chem. Phys. Lett. 135, 307–312.
24 Closs, G.L. and Forbes, M.D.E. (1987) J. Am. Chem. Soc. 109, 185–187.
25 Debus, R.J., Feher, G. and Okamura, M.Y. (1985) Biochemistry 25, 2276–2287.
26 Wraight, C.A. (1979) Biochim. Biophys. Acta 548, 309–327.
27 Tiede, D.M. and Dutton, P.L. (1981) Biochim. Biophys. Acta 637, 278–290.
28 Crespi, H.L. (1982) Methods in Enzymology, Vol. 88, pp. 3–5, ed. Packer, L., Academic Press, New York.
29 Hale, M.B., Blankenship, R.E. and Fuller, R.C. (1983) Biochim. Biophys. Acta 723, 376–382.
30 Okamura, M.Y., Isaacson, R.A. and Feher, G. (1975) Proc. Natl. Acad. Sci. USA 72, 3491–3495.
31 McElroy, J.D., Feher, G. and Mauzerall, D.C. (1972) Biochim. Biophys. Acta 267, 363–374.
32 Loach, P.A. and Hall, R.L. (1972) Proc. Natl. Acad. Sci. USA 69, 786–790.
33 Feher, G., Okamura, M.Y. and McElroy, J.D. (1972) Biochim. Biophys. Acta 267, 222–226.
34 Stehlik, D., Bock, C.H. and Petersen, J. (1989) J. Phys. Chem. 93, 1612–1619.
35 Leigh, J.S. and Dutton, P.L. (1974) Biochim. Biophys. Acta 357, 67–77.
36 Rutherford, A.W., Patterson, D.R. and Mullet, J.E. (1981) Biochim. Biophys. Acta 635, 205–214.
37 McIntosh, A.R., Manikowski, H. and Bolton, J.R. (1979) J. Phys. Chem. 83, 3309–3313.
38 McIntosh, A.R. and Bolton, J.R. (1979) Rev. Chem. Int. 3, 121–129.
39 Manikowski, H., McIntosh, A.R. and Bolton, J.R. (1984) Biochim. Biophys. Acta 765, 68–73.
40 Thurnauer, M.C. and Norris, J.R. (1980) Chem. Phys. Lett. 76, 557–561.
41 Thurnauer, M.C., Rutherford, A.W. and Norris, J.R. (1982) Biochim. Biophys. Acta 682, 332–338.
42 Thurnauer, M.C. and Clark, C.O. (1984) Photochem. Photobiol. 40, 381–386.
43 McCracken, J.L. and Sauer, K. (1983) Biochim. Biophys. Acta 724, 83–93.
44 McCracken, J.L. and Sauer, K. (1984) in Advances in Photosynthesis Research (Sybesma, C., ed.), Vol. I, pp. 585–588, Martinus Nijhoff/Dr. W. Junk Publishers, Dordrecht.
45 McCracken, J.L. (1983) Thesis, University of California, Berkeley, CA.
46 Broadhurst, R.W., Hoff, A.J. and Hore, P.J. (1986) Biochim. Biophys. Acta 852, 106–111.
47 Kirmaier, C., Holten, D., Debus, R.J., Feher, G. and Okamura, M.Y. (1986) Proc. Natl. Acad. Sci. USA 83, 6407–6411.
48 Crespi, H.L. (1977) Stable Isotopes in the Life Sciences, STI/PUB/442, pp. 111–121, Vienna.